Raman Imaging of Neoplastic Cells in Suspension

C. M. Creely[a*♦], S. Mercadal[a], G. Volpe[a], M. Soler[b], D. V. Petrov[a,c]
[a]ICFO - Institut de Ciencies Fotoniques, Mediterranean Technology Park, 08860 Castelldefels (Barcelona), Spain
[b]IBMB - Institut de Biologia Molecular de Barcelona, C. Jordi Girona 18-26, 08034 Barcelona, Spain
[c]ICREA - Institucio Catalana de Recerca i Estudis Avançat, Barcelona, Spain

ABSTRACT

The combination of Raman spectroscopy and Optical Tweezers has been used to trap living cells and collect information about their biochemical state. Cells can continue living in such traps for periods of hours, allowing acquisition of time resolved Raman spectra. However no spatial information can be acquired as the cells continue to rotate and move in the single beam trap.
Here we describe the development of Holographic Optical Tweezers (HOT) for the controlled movement of floating cells in order to construct their Raman images. Instead of a single trap, rapidly programmable multiple trapping points can be produced around the periphery of the cells to impede the rotational motion of the cell. By trapping and scanning the cell using HOT relative to a fixed Raman exciting laser, a point by point image of the cell can be constructed. We use an interactive program that permits us to position the trapping points relative to the live image feed we see from the microscope, using point and click. To demonstrate the possibilities of this technique images are shown of floating Jurkat cells.

Keywords: Raman imaging, Holographic Optical Tweezers, cancer cells

1. INTRODUCTION

Optical Tweezers (i.e. optical trapping of micron and submicron sized objects based on radiation pressure from a strongly focused light beam[1]) are a widely used tool in micromanipulation. One use of these tweezers has been the manipulation of living cells whose natural environment is to be in suspension. [2] The tightly focused laser beam required to form optical tweezers is usually formed through a high magnification microscope objective and is ideal for exciting Raman scattering from the trapped sample, making it straightforward to create a dual technique of OTRS (Optical Tweezers with Raman Spectroscopy), where the backscattered light is collected using the same microscope objective.

Optical techniques are advantageous for the study of biological samples where contamination could be an issue and Raman spectroscopy needs no special sample preparation, allowing cells and tissues to be studied in as close to in vivo conditions as possible. Other advantages of Raman spectroscopy are that it needs no special dyes or specific excitation wavelengths and also that a single scan contains information on all the different chemical components. In general near IR wavelengths are used for excitations chosen because of their low absorption in biological matter, furthermore wavelengths further from the UV/visible end of the spectrum create less background fluorescence, which can be a problem when trying to detect the much weaker Raman scattering. Raman spectroscopy has the advantage over IR absorption in that water, the primary component of living cells, only weakly Raman scatters.

The combined technique has been shown to be a non destructive method of analysis and has been the subject of numerous publications on living cells and biological particles see, for example [3,4,5,6,7]. It has previously been demonstrated that the combined technique is capable of monitoring dynamic cellular processes induced by temperature

♦ Caitriona.Creely@icfo.es; phone 0034 93 553 4076; fax 0034 93 553 4001; www.icfo.es

Optical Trapping and Optical Micromanipulation III, edited by Kishan Dholakia, Gabriel C. Spalding,
Proc. of SPIE Vol. 6326, 63260U, (2006) · 0277-786X/06/$15 · doi: 10.1117/12.679360

change. [8] Another application of OTRS was to investigate the biochemical response in a single cell to a chemically induced osmotic stress, the results of which were supported by previous biochemical assays, demonstrating the usefulness of this technique for real time studies of cell biochemistry.[9] Steps have been made towards the incorporation of this technique into a microfluidic system, using a dual-fibre setup, which can trap and acquire spectra from different points inside even large mammalian cells. [10]

In many cases it may not only be desirable to have time resolved information about biochemical changes taking place inside a cell but also to have information about where these changes are occurring. The technique of Raman imaging creates images of the chemical composition of the sample as a function of x and y coordinates.[11] Data are acquired either by scanning the laser beam back and forth across the sample, with a scanning galvanometer mirror or by scanning the sample across the laser beam, normally using a piezoelectric controlled stage, and acquiring the Raman spectrum at each point. The values of the intensity at a certain peak or peaks are plotted as a function of position. This has previously been used to create Raman images of cells which grow on substrates, and an example has been demonstrated where a chemical change signalling cell death was detected in a Raman image at an earlier time than was possible with a fluorescence image. [12]

The Raman imaging technique is suitable for cell lines which attach to a surface such as HeLa. The cells are naturally immobilised for the duration of the experiment, allowing us to image them. However the natural environment for other cells (such as blood cells) is to be in suspension. A single optical trap can restrict the Brownian motion of these types of cells to a certain extent, allowing us to trap a living cell for hours without damaging it. However the cell generally rotates in the trap and furthermore the concentration of power needed to trap an object larger than approximately 10 microns or so can severely damage a cell. Figure 1 shows a picture of a dividing yeast cell when trapped with one beam, and another picture shows the actual morphology of the cell which is not clearly visible when the cell is trapped. In this case Raman imaging cannot be performed because the cell aligns itself parallel to the axis of the Raman beam. This is the difficulty with attaining spatial information from a floating cells using only one beam as a tool.

We propose that a possible solution is to use multiple beams to trap the cell and move it relative to the fixed excitation point. This should not only allow for immobilising larger or dividing cells, but also distribute the power more evenly throughout the volume, limiting the damage to the cell. Holographic Optical Tweezers (HOT) can be used to provide such multiple tweezing sites which are programmable in real time, and have been used for trapping living cells. [13] The HOT traps and scans the cell back and forth across the focus of the stationary Raman excitation beam, taking a spectrum at each point and so builds up an image of the entire cell. In this way a Raman image of a floating cell can be constructed by plotting the concentration of various cellular components for each position inside the cell.[14] An advantage is that it requires no mechanical moving parts which could induce vibrations in the liquid medium.

In this paper Raman spectroscopy was used to create images of floating Jurkat cells. These are transformed human lymphocytes. A previous study was performed on normal lymphocytes comparing them with Jurkat cells, where OTRS was able to differentiate between the normal and cancerous cells.[15] However the larger size of the Jurkat cells made it difficult to trap and excite the cells using a single beam. Our system can overcome this and we use it to image Jurkat cells insolution.

2. EXPERIMENTAL SECTION

Our Optical Tweezers Raman spectroscopy (OTRS) system, shown in Figure 1, is as follows: it uses a diode laser (CrystaLaser) operating at 785 nm focused with a 100 x objective (N.A. = 1.2) into a sample holder placed on an inverse microscope (Olympus IX 51). This laser is used to excite the Raman spectra and the back scattered Raman light is collected with the same objective. This scattered light then passes through a holographic notch filter, cutting out most of the Rayleigh scattering, then through a confocal system and finally into a spectrometer (Spectra Pro 2500-I, Acton) equipped with a Princeton Instruments Spec-10 CCD cooled to -70°C. The entire microscope stage is in a heated enclosure to keep the temperature constant at 37° C.

The laser used for trapping cells was a 1064 nm Nd:Yag (Laser Quantum, max output 1W) modulated by reflection at an angle of 5 degrees off a liquid crystal Spatial Light Modulator (SLM) (Holoeye, LC-R 2500) with a resolution of 1024 x 768 pixels and a pixel size of 19 μm. The beam was expanded and collimated with lenses L_1 and L_2 so as to fill as much of the active area as possible and also to avoid any possible damage to the SLM surface caused by having the power density too high.

The diffracted beam from the SLM was passed through a telescope arrangement (L_3, L_4) to reduce the beam waist diameter to 6mm, the width of the objective aperture. The distance d from the SLM to the first lens of the telescope (L_3) and the distance from the second lens (L_4) to the confocal plane (Cp) were chosen such that the confocal plane coincided with the aperture of the microscope objective, and the distance between L_3 and L_4 was the sum of their focal distances.[16] The first diffracted order was selected using an aperture placed in front of L_4 to exclude any contribution from the zero order beam. Mirror M was positioned so as to centre the first order beam on it. Finally the position of the lens L2 was adjusted slightly along the axis of the beam to overlap the focus of the Raman excitation beam and the trapping beam in the z direction.

We downloaded a pre-existing LabView (National Instruments) program written to create multiple traps via holograms sent to the SLM which included an interface where the user can specify the number and position of traps using the mouse.[17] Extra functionality was added such as scanning the beams in a raster fashion, capturing the image from the microscope and most importantly integrating the movement with taking spectra at each point. For this part the program SpectraSense (Roper Scientific) was integrated into the LabView program as an ActiveX component.

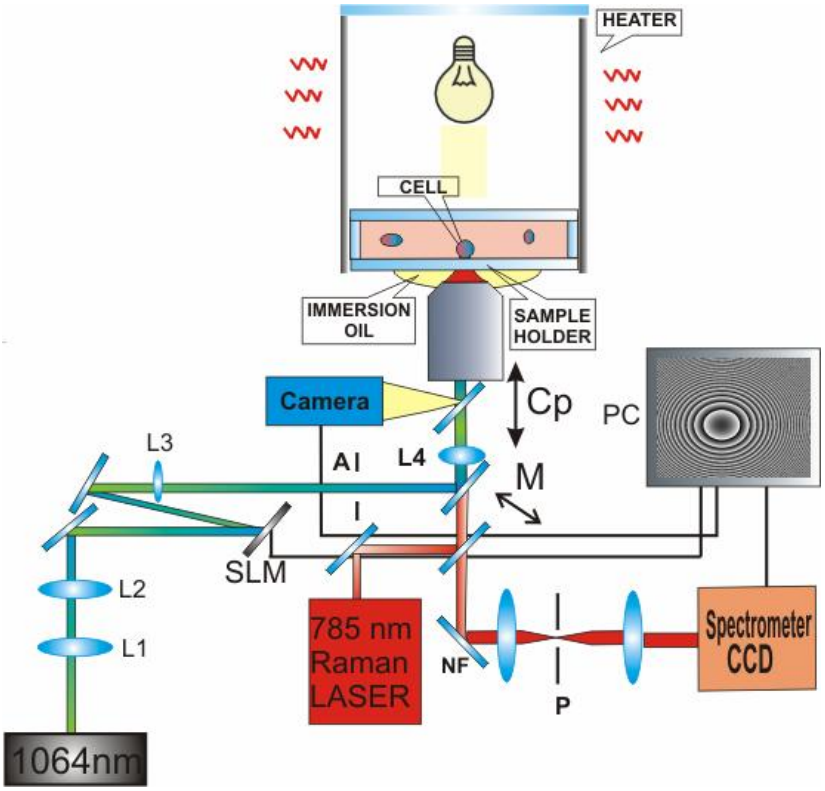

Fig. 1 HOT trapping set up with cells in a heated enclosure. L1-4: lenses used to collimate beam for SLM and reduce size to fill the microscope aperture. A: aperture which only passes first diffracted order. Cp: confocal plane. P: pinhole for confocal system.

Raman spectra were recorded over the range of 594 to 1696 cm^{-1}, which falls within the fingerprint region and provides the most information on the biological constituents of the cell. The 1064 nm laser was used to scan each cell with respect to the stationary 785 nm laser beam in order to acquire spectra at different points inside the floating cell. The power of the 1064 nm laser measured at the focal plane was 7.5 mW, which in our case we used to produce two beams of equal intensity for trapping each cell. The dwell time at each point was 90 s, giving a total time for each scan of

approx. 54 minutes, using 900 μW of excitation power at the sample plane. The step sizes were 1 microns and scan areas varied from experiment to experiment, according to the size of the cancer cell.

The cells used were Jurkat Clone E6-1, T-lymphocytes cultured in RPMI in suspension with 10% FBS under standard conditions. Jurkat cells are a cell line derived from human T-cell leukemia. Cells were trapped inside a custom-made sample holder using a 100 μm fused silica cover slip to reduce signal which is normally associated with glass sample holders. The holder was cleaned with pure ethanol and allowed to air dry before use. A cover slip was placed on top to prevent liquid evaporation during the experiments.

Numerous spectra (60 s acquisition) of live and apoptotic Jurkat cells were taken and analysed using the normal OTRS setup without using the HOT. These data were taken with the power of the Raman beam 2.8 mW. This data first had cosmic rays removed, then a baseline fitted to remove fluorescence background. The subtracted spectrum subsequently had a Savitsky-Golay smoothing function applied (2nd order, 13point). Raman images were created using peaks that appeared in these spectra.

Data used for the Raman images first had cosmic rays removed and was then smoothed by Savitsky-Golay (2nd order, 9 pt smoothing). This analysis of the spectra for the Raman images was automated by a custom-made program called RamImage, based on MatLab 7®. The program integrated the cosmic ray removal, Savitsky-Golay smoothing, spectra plotting and image plotting for peaks as a function of xy coordinate into a single graphical interface.

HOT: When a monochromatic beam is focused by a lens the electric field of the incident wave, $E^{in}(\vec{r})$, and the one at the focal plane, $E^{f}(\vec{\rho})$, are related by the two dimensional Fourier transform pair:

$$E^{f}(\vec{\rho}) = \frac{k}{2\pi f} e^{i\theta(\vec{\rho})} \int d^2 r \; E^{in}(\vec{r})\, e^{-ik\vec{r}\cdot\vec{\rho}/f} = \Im\left\{E^{in}(\vec{r})\right\}, \tag{1}$$

$$E^{in}(\vec{r}) = \frac{k}{2\pi f} \int d^2 r \; e^{-i\theta(\vec{\rho})} E^{f}(\vec{\rho})\, e^{ik\vec{r}\cdot\vec{\rho}/f} = \Im^{-1}\left\{E^{f}(\vec{\rho})\right\}, \tag{2}$$

where f is the focal length of the lens and $k = 2\pi/\lambda$ is the wave number of the incident light. Thus, shaping the phase and amplitude of the incident electric field permits one to shape the E-field at the focal plane. Since optical trapping relies on the beam's intensity and not on its phase, it is possible to modulate only the phase of the incident beam, without changing the amplitude, which would involve a reduction in the intensity of the beams.

Only a small number of trapping points were needed for the experiment; however they need to be able to change rapidly so that the cell doesn't have time to escape from the trap. This can be described in the focal plane as the following convolution:[18]

$$E^{f}(\vec{\rho}) = E_0^{f}(\vec{\rho}) \otimes \frac{1}{\sqrt{N}} \sum_{i=1}^{N} \delta^{(2)}(\vec{\rho} - \vec{\rho}_i), \tag{3}$$

where $E^{f}(\vec{\rho})$ is the desired electric field at the focal plane, $E_0^{f}(\vec{\rho})$ is the original electric field at the focal plane, N is the number of points and $\delta^{(2)}(\vec{\rho} - \vec{\rho}_i)$ is the two dimensional delta function centered in $\vec{\rho}_i$. Operating the inverse Fourier transform, the required expression for the input electric field is:

$$E^{in}(\vec{r}) = \frac{2\pi f}{k} E_0^{in}(\vec{r}) \times \frac{1}{\sqrt{N}} \sum_{i=1}^{N} \exp(-ik\vec{r}\cdot\vec{\rho}_i) = E_0^{in}(\vec{r}) \exp\left[i\Phi^{in}(\vec{r})\right], \tag{4}$$

where $E^{in}(\vec{r})$ is the desired input electric field and $E_0^{in}(\vec{r})$ is the original input electric field and $\Phi^{in}(\vec{r})$ represents the needed phase modulation of the input wave front. Taking into account the effect of the telescope (lenses L_1 and L_2 in Figure 1) it is possible to calculate the hologram that has to be projected onto the Spatial Light Modulator (SLM):

$$\Phi^{SPM}(x,y) = \frac{256}{2\pi} angle\left\{\sum_{i=1}^{N} \exp(-ik\vec{r}\cdot\vec{\rho}_i)\right\}, \tag{5}$$

where the term $256/2\pi$ is a normalization constant between the value of the angle expressed in radians and the value of the pixel and angle is chosen with the determination within (0,2π). It is possible to directly calculate the values of the

hologram without need for Fourier transform and adaptive algorithms. This reduces the computation complexity of the algorithm from O(n ln n), for the case that involves a 2D-FFT, to (O(n)), where *n* is the number of pixels to be calculated. In particular, since the calculation of the phase of the hologram requires less then 1s on a 2GHz PC, this allows almost real-time reconfiguration of the optical trap configuration.

3. RESULTS AND DISCUSSION

Figure 2 shows stills from a movie taken of a cell trapped by multiple beams compared with those trapped by a single beam. The latter case shows more rotation in the trap, showing that a more stable trapping configuration can be achieved with multiple beams. This is despite the fact that the overall power of the single trap is slightly more than that of the double trap as a result of ghost traps formed in the multiple beam case, which divert power away from the main traps.

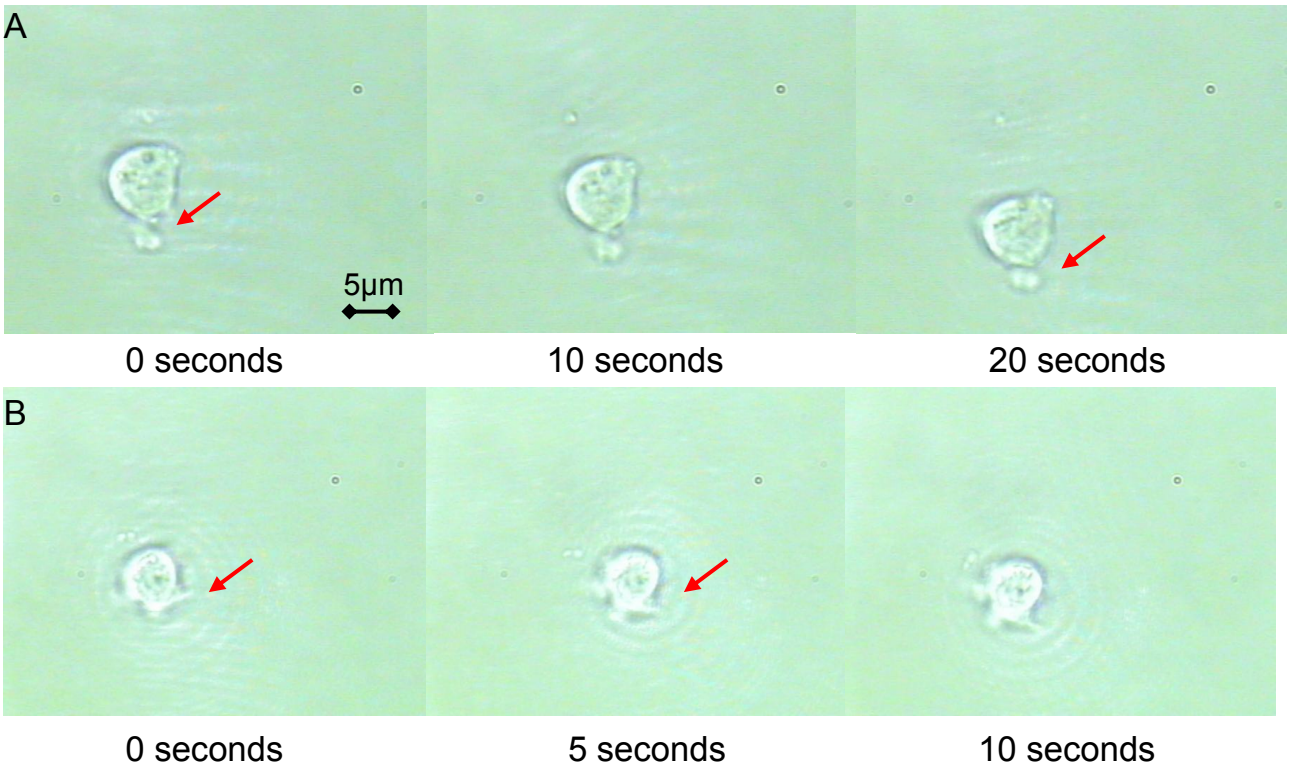

Fig. 2. The upper row of photos are stills from a movie showing the HOT movement of a Jurkat cell using two beams. After 20 seconds the feature seen at the bottom of the cell (indicated by the arrow) is still in the same position although the cells itself has been scanned through the liquid. The lower three stills show a cell where only one beam was used to trap. The cells shows rotation in this case after only 5 sec.

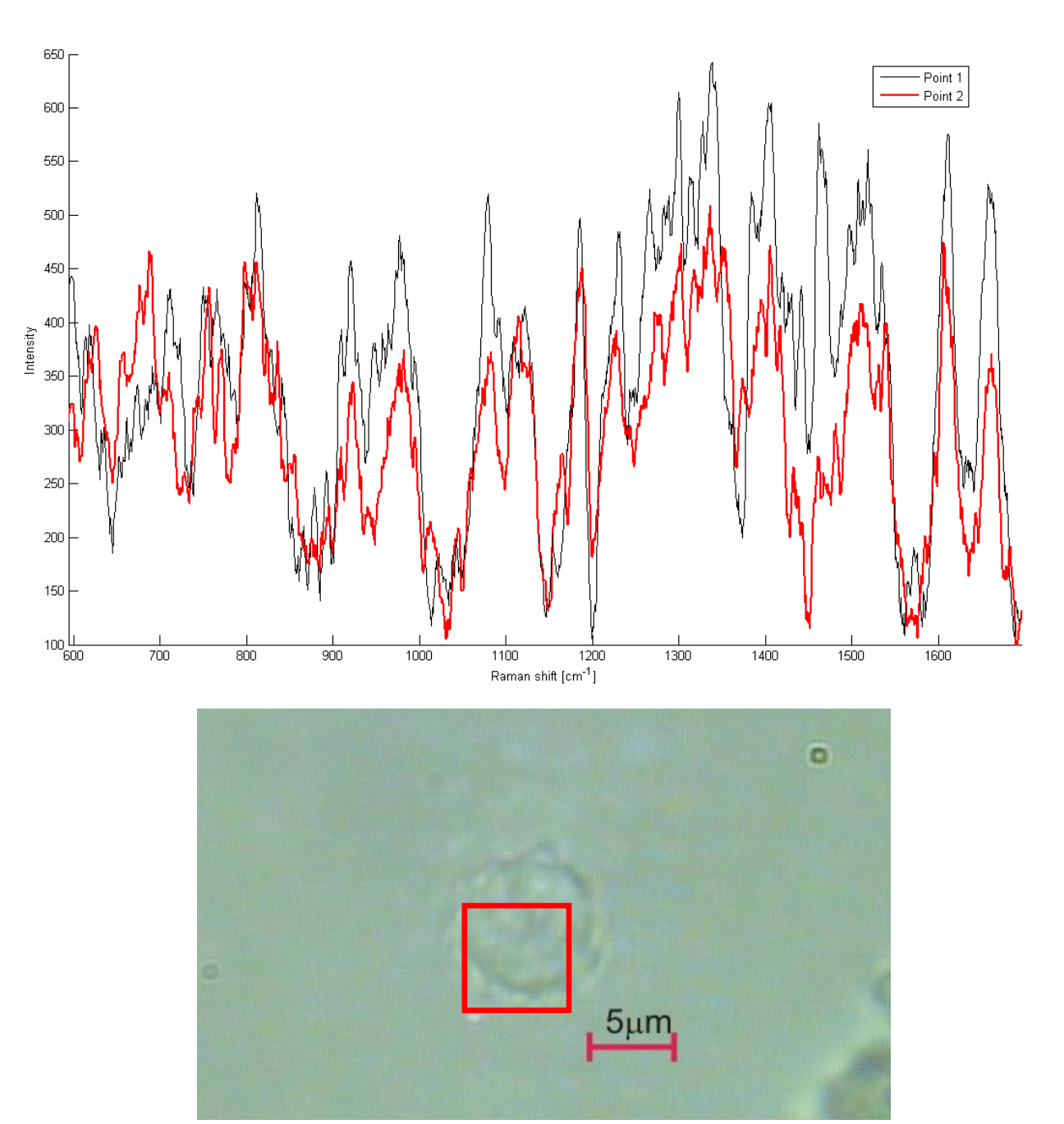

Fig. 3. (a) Jurkat cell in suspension with excitation beam showing as a red dot to the lower left hand corner. Red box shows scan area. (b) Spectrum from different points inside the cell, 60s acquisition.

Figure 3 shows spectra taken from different points within a Jurkat cell showing the point-to-point variation of the Raman signal. Peaks can be assigned to constituents of the cells such as proteins, DNA etc. The spectra shown had a baseline fitted to remove background fluorescence and were smoothed. These peaks were then used to construct the Raman images. Peaks assignments used for imaging were assigned as follows: 1003 cm^{-1} (Phenylalanine), 725 cm^{-1}(Adenine), 1208 cm^{-1} (Amide III) and 1447 cm^{-1} (CH_2 def) from reference [15].

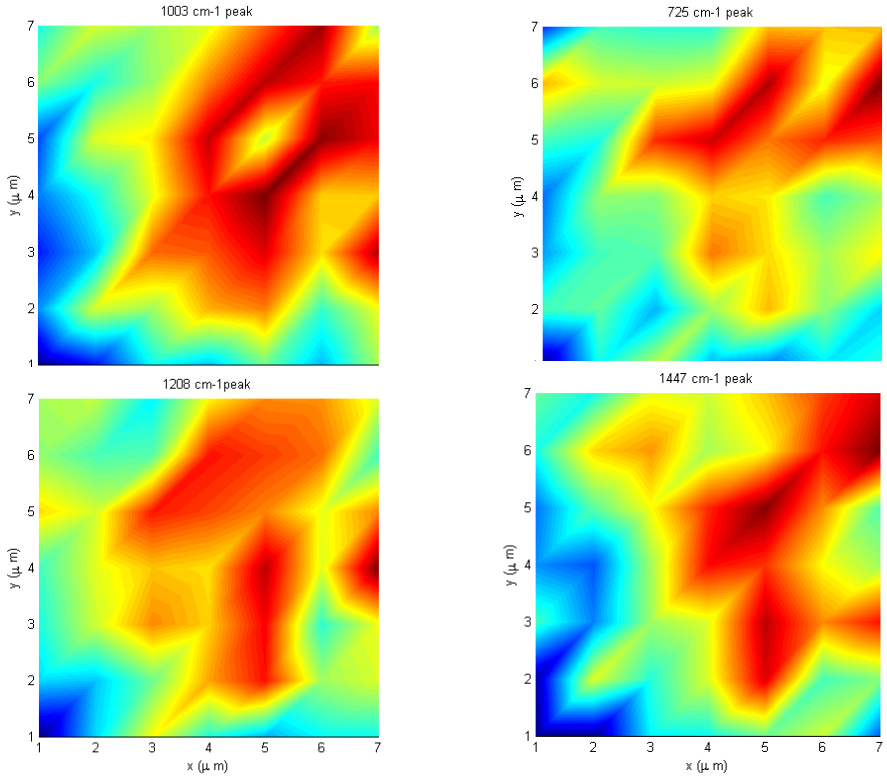

Fig. 4. Raman images of a living Jurkat cell in suspension with 4 different bands imaged. A 6x6x1 micron scan was performed. Bands imaged are 1003 cm^{-1} (Phenylalanine), 725 cm^{-1}(Adenine), 1208 cm^{-1} (Amide III) and 1447 cm^{-1} (CH_2 def).

Figure 4 show false colour images of concentrations of different constituents inside a single living Jurkat cell. An area of 6x6 microns was scanned with a step size of 1 micron. The cell was still intact after the measurement. We can readily see a different distribution for a single constituent within the cell and also between the four separate constituents. Chan et. al. acquired spectra from different points inside Jurkat cells which had settled onto a glass cover slip.[15] They noticed quite a low spatial variation for these spectra which they attributed to the large nucleus/cytoplasm ratio, meaning that the nucleus was constantly being probed. Our spectra in Figure 3 show comparatively greater changes. One reason could be that the cells imaged on the cover slip should exhibit a higher background, which may obscure some of the spectral variations that we see with the HOT system, making this an advantage of our system.

These images are an example of Raman imaging of floating living cells using HOT to immobilise and manipulate the cells with respect to the exciting beam. Some issues have to be addressed however. The exciting Raman laser also contributes a trapping force which means that with the current experimental setup the excitation power must be reduced greatly in order not to interfere with the HOT. This gives rise to long acquisition times. An altered scheme where a second 785 nm laser propagating anti-parallel to the original 785 nm beam could in theory cancel out the scattering force, thus the Raman excitation power could be increased to have a shorter total scan time. This 2nd 785 nm beam would contribute to the Raman scattering, and the confocal aperture (see Figure 1) would still select only the scattering from the confocal volume. It could be beneficial to trap using 785 nm light and excite using a lower wavelength that does not affect the Raman spectrum. This would yield a larger Raman spectrum, and we feel that 785 nm is a less damaging wavelength for living cells than 1064 nm. In order to achieve greater spatial resolution or whole floating cell images the Raman signal has to be increased in order to compensate for the extra scanning points needed. A possible problem that can arise when trying to trap and image apoptotic floating cells is that the extra sources of laser intensity needed for trapping can be too damaging for some cells (at 1064 nm), and using too high a power can perforate the membrane and induce blebbing.

The HOT real-time manipulation system is compatible with other imaging methods, for instance with multiphoton imaging using different lasers for trapping and imaging. Two-photon fluorescence images have been produced of trapped single yeast cells by moving an external lens to change the position of the trapped cell.[19] The holographic tweezers system offers greater flexibility and numerous points can be created instantly. This could allow cell-cell interactions to be studied in real-time by multiphoton imaging combined with HOT.

ACKNOWLEDGEMENTS

This research was carried out in the framework of ESF/PESC (Eurocores on Sons), through grant 02-PE-SONS-063-NOMSAN, and with the financial support of the Spanish Ministry of Science and Technology (FIS2005-02129). It was also supported by the Departament d'Universitats, Recerca i Societat de la Informaciò and the European Social Fund.

[1] A. Ashkin, "Acceleration and trapping of particles by radiation pressure," *Phys. Rev. Letts.* 24, 156 -159 (1970).
[2] A. Ashkin, J. M. Dziedzic, T. Yamane, "Optical trapping and manipulation of single cells using infrared laser beams," *Nature* 330**,** 769-771 (1987).
[3] C. Xie, M. A. Dinno, Y. Li, "Near-infrared Raman spectroscopy of single optically trapped biological cells," *Opt. Lett.* 27, 249-251 (2002).
[4] J. L. Deng, Q. Wei, M. H. Zhang, Y. Z. Wang, and Y. Q. Li, "Study of the effect of alcohol on single human red blood cells using near-infrared laser tweezers raman spectroscopy," *J. Raman Spec.* 36, 257-261 (2005).
[5] G. P. Singh, G. Volpe, C. M. Creely, H. Grötsch, I. M. Geli, D. Petrov, " The lag phase and G1 phase of a single yeast cell monitored by Raman microspectroscopy", *J. Ram. Spec.* (In press)
[6] R. Gessner, C. Winter, P. Rösch, M. Schmitt, R. Petry, W. Kiefer, M. Lankers and J. Popp, "Identification of Biotic and Abiotic Particles by Using a Combination of Optical Tweezers and In Situ Raman Spectroscopy", *ChemPhysChem* 5, 1159-1170 (2004).
[7] J. W. Chan, A. P Esposito, C. E. Talley, C. W. Hollars, S.M. Lane, T. Huser, "Reagentless identification of single bacterial spores in aqueous solution by confocal laser tweezers", *ChemPhysChem* 5 1159-1170 (2004)
[8] C. G. Xie, Y. Q. Li, W. Tang, and R. J. Newton, "Study of dynamical process of heat denaturation in optically trapped single microorganisms by near-infrared Raman spectroscopy," *J. Appl. Phys*. 94, 6138-6142 (2003).
[9] G. P. Singh, C. M. Creely, G. Volpe, H. Grötsch, and D. Petrov, "Real-time detection of hyperosmotic stress response in optically trapped single yeast cells using Raman Microspectroscopy," *Anal. Chem.* 77, 2564-2568 (2005).
[10] P. R. T. Jess, V. Garcés-Chávez, D. Smith, M. Mazilu, L. Paterson, A. Riches, C. S. Herrington, W. Sibbett and K. Dholakia, "Dual beam fibre trap for Raman microspectroscopy of single cells," *Opt. Express* 14 5779-5791 (2006).
[11] N. Uzunbajakava, A. Lenferink, Y. Kraan, B. Willekens, G. Vrensen, J. Greve, C. Otto "Nonresonant Raman Imaging of Protein Distribution in Single Human Cells," *Biopolymers* 72, 1-9 (2003).
[12] Y. Huang, T. Karashima, M. Yamamoto, T. Ogura, H. Hamaguchi, "Raman spectroscopic signature of life in a living yeast cell", *J. Ram. Spec.* 35, 525-526 (2004).
[13] V. Emiliani, D. Cojoc, E. Ferrari, V. Garbin, C. Durieux, M. Coppey-Moisan, and E. Di Fabrizio, "Wave front engineering for microscopy of living cells," *Opt. Express* 13, 1395-1405 (2005).
[14] C. M. Creely, G. Volpe, G. P. Singh, M. Soler, and D. V. Petrov, "Raman imaging of floating cells," *Opt. Express* 13, 6105-6110 (2005).
[15] J. W. Chan, D. S. Taylor, T. Zwerdling, S. M. Lane, K. Ihara, and T. Huser, "Micro-Raman Spectroscopy detects individual Neoplastic and normal Hematopoietic cells," *Biophys. J.* 90, 648-656 (2006).
[16] E. Fällman and O. Axner, "Design for fully steerable dual-trap optical tweezers," *Appl. Opt.* 36 2107-2113 (1997)
[17] J. Leach, K. Wulff, G. Sinclair, P. Jordan, J. Courtial, L Thomson, G. Gibson, K. Karunwi, J. Cooper, Z. J. Laczik and M. Padgett, " Interactive approach to Optical Tweezers Control," *Appl. Opt.* 45, 897-903 (2006).
[18] G. C. Spalding, M. T. Dearing, S. A. Sheets, and D. G. Grier, "Computer-generated holographic optical tweezer arrays," *Rev. Sci. Instr.* **72,** 1810-1816 (2001).
[19] M. Goksor, J. Enger, D. Hanstorp, "Optical manipulation in combination with multiphoton microscopy for single-cell studies," *Appl. Opt.* 43, 4831-4837 (2004).